Chemical Science

ROYAL SOCIETY OF CHEMISTRY

EDGE ARTICLE

View Article Online
View Journal

Cite this: DOI: 10.1039/d6sc00316h

All publication charges for this article have been paid for by the Royal Society of Chemistry

Received 13th January 2026
Accepted 3rd April 2026

DOI: 10.1039/d6sc00316h

rsc.li/chemical-science

Bridging Lewis acidic antimony centers with electron-withdrawing carborane cages

Victoria P. Rubio, [a] McKinley H. Durham,[a] Matthew Scurria, [a] Tyler A. Kerr, [a] Osvaldo Gutierrez *[a] and Alexander M. Spokoyny *[ab]

While fluorinated carbon-based electron withdrawing substituent groups are commonly employed when strengthening the Lewis acidity of group 15 organometallic compounds, we exploit an alternative approach by leveraging the electron-withdrawing properties of the carbon vertices of three-dimensional icosahedral boron clusters, known as carboranes. Here, we report the synthesis of C-bound *ortho*-carborane bridged antimony(III) species, which can be conveniently oxidized to their antimony(V) counterparts using *o*-chloranil. The corresponding antimony(V) species have proven to strongly bind to small molecules showing that with the aid of bulky C-bound carborane groups, antimony(V) centers have enhanced Lewis acidic properties. This improved Lewis acidity is confirmed *via* binding studies and computational analysis, which together highlight the reactivity of accepting σ^* orbitals, commonly referred to as sigma holes.

Introduction

A well-established strategy for modulating Lewis acidity in main group-based compounds centers on using carbon-based substituents to tune both steric and electronic environments. Specifically, perfluoroaromatic substituents have been known for several decades as strong electron-withdrawing moieties, which when appended to a certain atom (*e.g.*, B, Al, Si, Hg) can confer substantial Lewis acidity in the resulting species (Fig. 1).[1–5] In 1991, Hawthorne reported a class of mercury-based macrocycles containing C–Hg-bound carborane-based ligands which exhibited unprecedented Lewis acidic properties stemming from electron-poor Hg(II) sites.[6,7] This work raises the question of whether C-bound carborane clusters can exhibit electron-withdrawing properties comparable to those of perfluoroarenes. Over the next two decades, subsequent studies by several groups showed that when *ortho*- and *meta*-carborane (subsequently abbreviated as *o*- and *m*-carborane, respectively) clusters are C-bound to other heteroatoms including phosphorus,[8a,b] sulfur,[8c,d] carbon,[8e] selenium,[9] iodine,[10] boron,[11] and most recently tin,[12] they exhibit electron-withdrawing properties that can surpass the inductive effect of the pentafluoroaryl group (Fig. 1).

Among the existing main group Lewis acids, heavy pnictogen (Sb, Bi) compounds remain relatively underexplored compared to their organoborane counterparts.[13–15] Specifically, Sb(V) and Bi(V) compounds can engage in noncovalent binding due to the presence of a low-lying sigma star (σ^*) orbital on the heavy atom. These binding interactions are normally termed as pnictogen (Pn) bonding. Analogous to halogen and chalcogen bonding, these interactions can be enhanced by the nature of the substituent directly attached to the Pn(V) site which deepens the sigma-hole and lowers the energy of the accepting σ^* orbital, thus enhancing Lewis acidity.[16–19a–e]

Inspired by Pn(V) species and the superior ligand properties of icosahedral carboranes, we sought to combine both features in the design of new antimony-based Lewis acids. In a series of seminal papers, Gabbaï and co-workers have recently advanced the field of Lewis acidic organostiboranes using perfluoroaryl substituents.[20–22] Specifically, they reported a series of Sb(V) compounds whose Lewis acidity is reflected in fluorine ion affinity (FIA) values approaching 400 kJ mol^{-1}. Here we demonstrate how replacing the perfluoroaryl moiety with an *o*-carboranyl substituent results in a 40–50 kJ mol^{-1} increase in FIA. This is further reinforced by experimental measurements using the ^{31}P chemical shift of triethylphosphine oxide (Et_3PO) in the presence of Sb(V) compounds, as well as solution-based fluoride titrations.[23,24] Overall, this work highlights how carboranes can act as powerful electron withdrawing substituents surpassing perfluoroaryls in the context of Pn(V) chemistry.

Results and discussion

To date, only one report describes an exopolyhedral carborane C–Sb bond, where Bregadze and co-workers claimed the successful synthesis of Sb(2-Ph-*o*-carborane)$_3$ on the basis of elemental analysis and melting point data, obtained by heating

[a]*Department of Chemistry and Biochemistry, University of California, Los Angeles, 607 Charles E. Young Drive East, Los Angeles, California 90095, USA. E-mail: spokoyny@ucla.edu; o.gutierrez@ucla.edu*

[b]*California NanoSystems Institute, University of California, Los Angeles, Los Angeles, California 90095, USA*

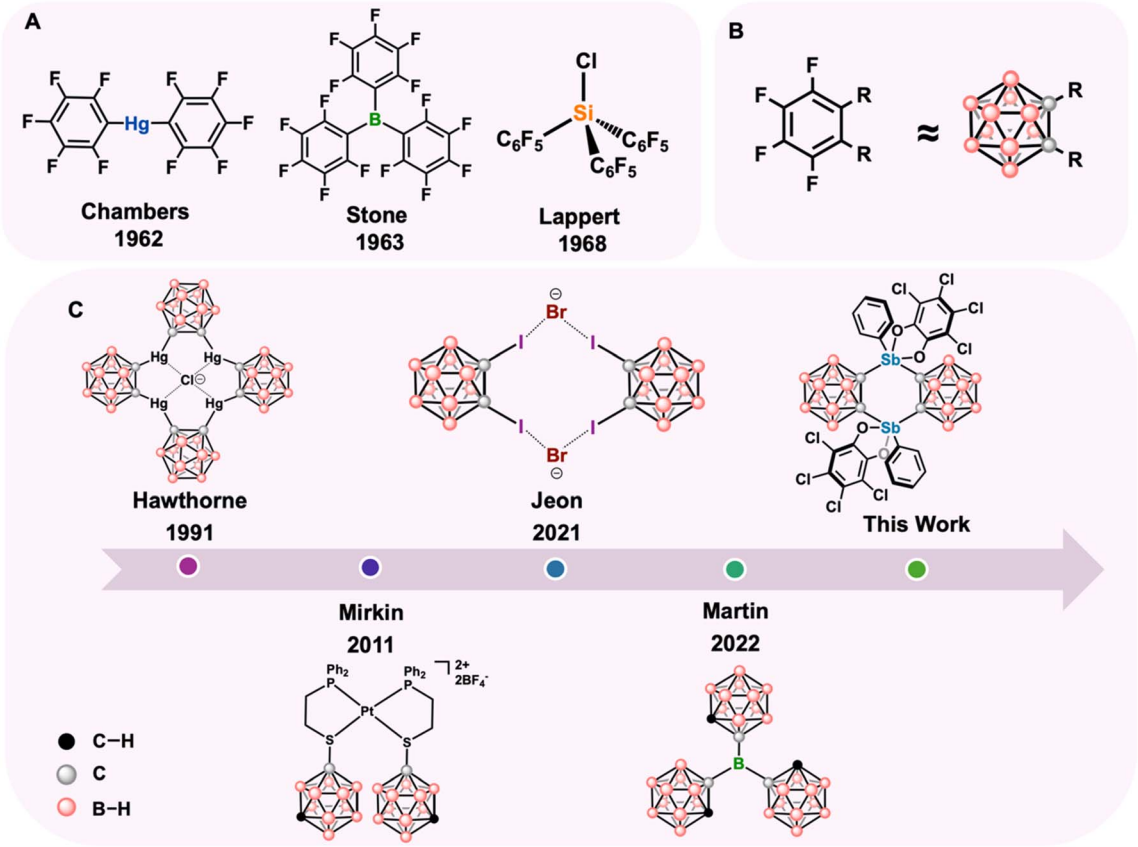

Fig. 1 (A) Select, early examples of perfluoroaryl-stabilized main-group species. (B) Comparison of perfluoroaryl and C-bound carborane substituents as inductively withdrawing motifs. (C) Representative advances in carborane-based architectures demonstrating extreme electron-withdrawing properties of C-bound icosahedral carboranes.

1-Li-2-Ph-*o*-carborane in neat $SbCl_3$.[25] In order to determine the general synthetic feasibility of attaching two Sb(III) substituents onto the carbon vertices of *o*-carborane, we have chosen dilithiated *o*-carborane as a potential reagent of choice that can engage in a nucleophilic substitution with antimony-based electrophiles. A solution of $SbCl_2Ph$[26] dissolved in dry dichloromethane (DCM) is added to a suspension of freshly prepared dilithiated *o*-carborane, and the resulting reaction mixture is left stirring at room temperature for 12 hours; *in situ* ^{11}B NMR spectroscopy indicates full consumption of the starting material. Following workup, the crude product material is recrystallized in benzene affording spectroscopically pure compound **1a**, consistent with the multinuclear NMR (^{1}H, $^{13}C\{^{1}H\}$, ^{11}B, $^{11}B\{^{1}H\}$) spectroscopy.

Specifically, the NMR spectra confirm the bridged architecture, as evidenced by the disappearance of the characteristic *o*-carborane C–^{1}H resonance at 3.20 ppm in the ^{1}H NMR spectrum and the corresponding integration of the B–H and aromatic regions. Finally, X-ray crystallographic studies on the single crystals of **1a** grown in benzene unequivocally support the proposed structural model where two Sb(III) centers are connected with two C-bound *o*-carboranyl ligands, resulting in the formation of a six-membered Sb-containing heterocycle (Fig. 2).

We found that by changing the antimony precursor from $SbPhCl_2$ to the $SbPh_2Cl$ species, the C-bound *o*-carboranyl Sb(III) species **2a** can be accessed, where only one *o*-carborane ligand bridges two Sb(III) sites. This compound was synthesized in 62% yield using a procedure similar to the synthesis of **1a** (see SI). Heteronuclear NMR spectroscopy and single crystal X-ray structural characterization are fully consistent with the proposed structural formulation of **2a** (Fig. 2). The ability to prepare both **1a** and **2a** allowed us to explore the steric and electronic effects imposed on the heavy pnictogen center by the *o*-carboranyl moieties. While the ^{11}B NMR spectrum for **1a** and **2a** is less informative due to its broadening, its noticeably distinct features compared to the starting material further support the formation of **2a**. The broadening is ascribed to newly introduced fluxionality in **2a** due to possible rotation of the phenyl rings.[27–29] Low temperature ^{11}B NMR spectroscopy experiments at −20 °C further support this hypothesis with the low temperature spectrum undergoing significant sharpening. In order to establish this benchmarking, access to the corresponding Sb(v) species is required, as enhanced Lewis acidity is associated with a higher oxidation state metalloid (Sb) center.[30–33] Gabbaï and co-workers have previously developed an elegant approach that cleanly oxidizes Sb(III) aryl compounds to their Sb(v) congeners using *o*-chloranil. Gratifyingly, oxidation

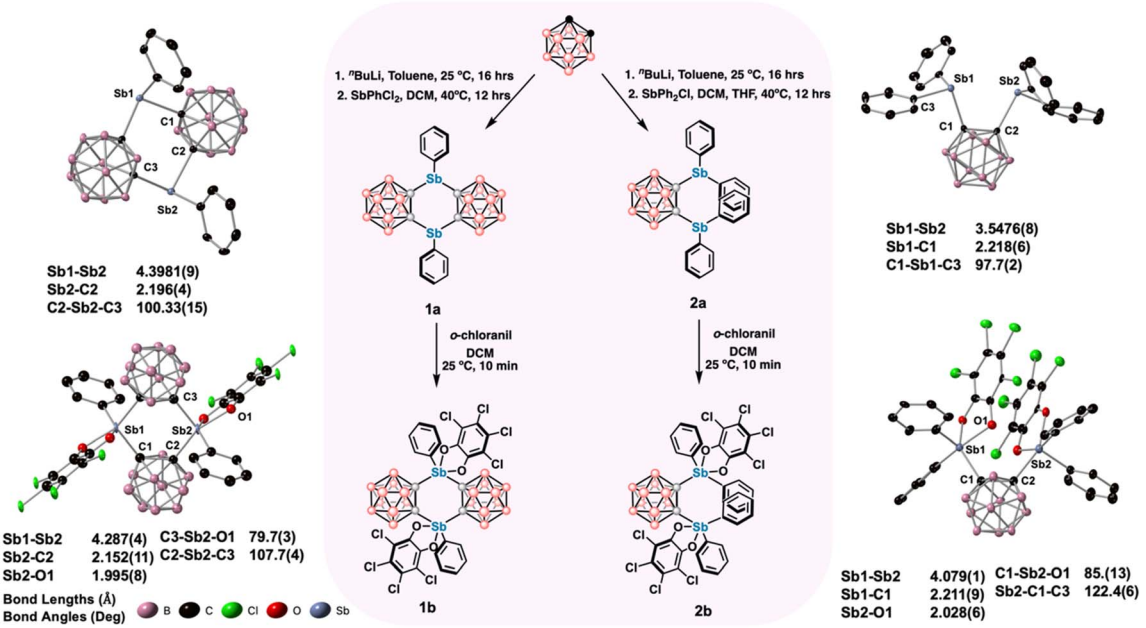

Fig. 2 Center: Synthetic routes to *mono*(carboranyl) and *bis*(carboranyl) stiboranes *via* *o*-carborane lithiation, electrophilic substitution with $SbPh_2Cl$ or $SbPhCl_2$, and oxidation with *o*-chloranil. Left: solid-state structures of **1a** and **1b**. Right: solid-state structures of **2a** and **2b** showing the corresponding geometric and bonding changes upon oxidation to Sb(v). Thermal ellipsoids drawn at 50%.

of **1a** and **2a** with *o*-chloranil afforded the corresponding Sb(v) species, **1b** and **2b**.[34,35] The oxidation proceeds rapidly at room temperature, signified by the disappearance of the red *o*-chloranil color providing a convenient visual indicator when the conversion is complete. Following oxidation, **1b** precipitates as an orange solid whereas **2b** remains in an orange solution. Multinuclear NMR spectra of both products are distinct from the parent Sb(III) species, and new resonances in the ^{13}C spectrum of the aryl region are consistent with incorporation of the *o*-chloranil diolate ligand at the newly formed Sb(v) sites. Single-crystal X-ray structures of both compounds confirm the change from trigonal pyramidal coordination at Sb(III) to a distorted trigonal bipyramidal geometry at Sb(v), characteristic of an organostibane(V) center when bound to *o*-chloranil.[36,37]

Apart from the distinct geometry change, it is noteworthy to mention the metalloid bond distances between the Sb(III) and Sb(v) species. In **1a**, the Sb(1)–Sb(2) distance is 4.398(9) Å, with a nearly symmetric Sb(1)–C(1) bond length of 2.196(4) Å to the bridging *o*-carborane cage. Upon oxidation to **1b**, the Sb(1)–Sb(2) distance contracts to 4.287(4) Å likely due to the electron deficient nature of the Sb(v) centers, resulting in shorter bonds. Additionally, the crystal structure shows Sb–O bond distances of 1.995(8) Å and 2.040(8) Å. In the context of **2a**, the mono(-carboranyl) species, the Sb(1)–Sb(2) distance is shorter at 3.5476(8) Å, and the Sb(1)–C(1) bond length is slightly longer (2.218(6) Å), consistent with reduced steric congestion. Upon oxidation to **2b** the Sb–Sb separation increases significantly to 4.079(1) Å and the Sb(2)–O(1) bond is slightly longer (2.047(3) Å) than **1b**. When comparing **1b** and **2b** to similar pnictogen bridged species, this *o*-carborane bridged Sb–Sb pocket is quite large. Gabbaï and co-workers reported a Sb(1)–Sb(2) distance of 3.817 Å in $(o\text{-}Cl_4C_6O_2)_2Sb_2(C_6F_4)(C_6H_5)_4$, in which the Sb(1)–Sb(2) atoms are bridged by a perfluoroaryl ligand.[22] In our analogous compound **2b**, we show a longer Sb(1)–Sb(2) distance (4.079(1) Å) which allows for a more accessible Lewis acidic site for small molecule binding.

The Lewis acidity of oxidized stiboranes **1b** and **2b** was quantified using the Gutmann–Beckett (GB) method, a standard probe of Lewis acid–base interactions that monitors coordination of triethylphosphine oxide (Et_3PO) *via* its ^{31}P NMR chemical shift.[23,24] Upon addition of one equivalent of Et_3PO to **2b** in dichloromethane, the ^{31}P NMR resonance shifts from 50.0 ppm (free Et_3PO) to 66.6 ppm ($\Delta\delta$ = 16.6 ppm), which indicates coordination of Et_3PO to the antimony center. Under identical conditions, when **1b** is exposed to Et_3PO, a new ^{31}P NMR shift for the resulting complex is observed at 71.6 ppm, which corresponds to a $\Delta\delta$ of 21.6 ppm. While we were unable to obtain a diffraction quality crystal to confirm the structural identity of the **1b**-Et_3PO adduct, *in situ* NMR spectroscopic analysis supports the identity of this species as **1c** (Fig. 3A). On the other hand, vapor diffusion of **2b** treated with Et_3PO resulted in the formation of diffraction quality crystals. X-ray crystallographic analysis of the adduct **2b**-Et_3PO reveals terminal, monodentate Sb–O coordination (Sb1–O1 = 2.178(2) Å). The elongated Sb–O distance between Et_3PO and the antimony center relative to a standard single Sb–O bond (~2.03 Å) implies steric hindrance from the carborane cage and neighboring aryl groups.[38,39] Upon addition of two equivalents of Et_3PO to **1b**, two discrete ^{31}P NMR resonances (70–75 ppm) emerge, signifying that the Sb sites are inequivalent following the initial binding of Et_3PO (SI, Fig. S34).

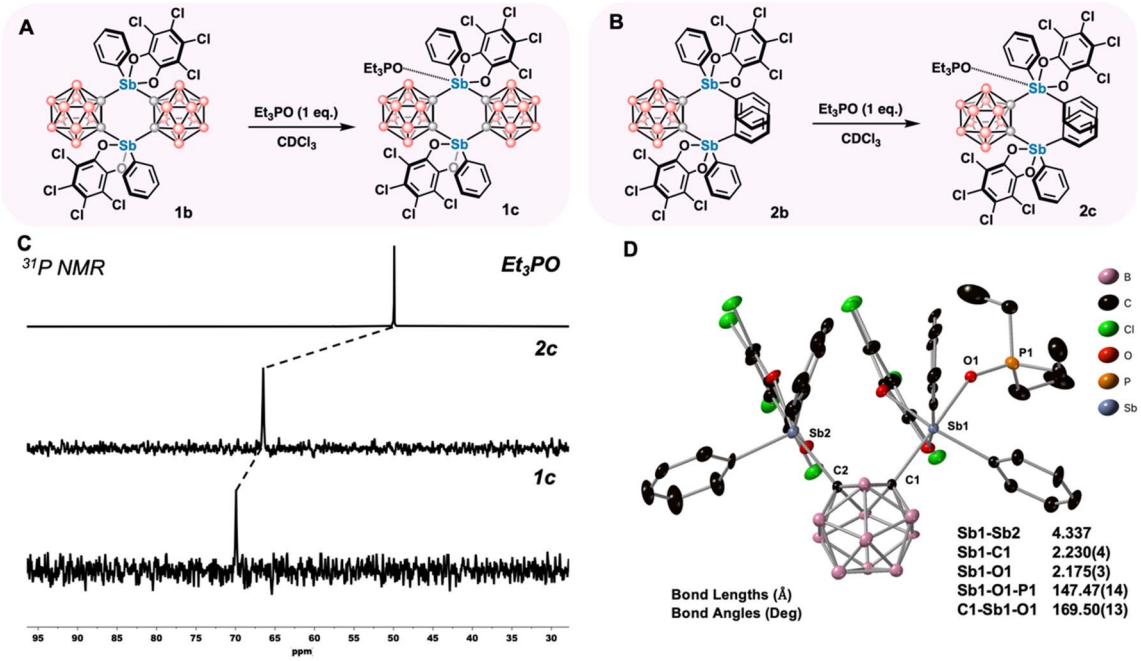

Fig. 3 (A and B) Gutmann–Beckett titrations of Sb(v) complexes **1b** and **2b** with 1 equiv. Et_3PO in $CDCl_3$, forming adducts **1c** and **2c**. (C) ^{31}P NMR spectra showing downfield coordination shifts for Et_3PO upon binding to **1b** and **2b**. (D) Solid-state structure of **2c** with selected bond lengths and angles, highlighting Sb–O coordination and the resulting geometric changes.

Based on established benchmarks for Lewis acids, the magnitude of the ^{31}P NMR shift upon coordination of Et_3PO can be correlated with Lewis acidity.[40–42] For example, $Sb(C_6F_5)_3(-O_2C_6Cl_4)$ has been reported as a strong Lewis acidic stiborane on the Gutmann–Becket scale, producing a ^{31}P NMR signal at 74 ppm upon binding Et_3PO while free Et_3PO results in a ^{31}P NMR shift of 55 ppm.[46] This correlation provides a convenient spectroscopic handle for comparing Lewis acidity across main group centers, particularly with the pnictogen series.[43–45] Therefore, the observed GB results for both **1b** and **2b** indicate strong Lewis acidity when Sb is bound to the strongly electron withdrawing group, C-bound *o*-carboranyl. In addition, the presence of two C-bound *o*-carboranyl moieties in **1b** enhances the Lewis acidity compared to **2b**. The ~5 ppm ^{31}P NMR shift increase from **2b** to **1b** when bound to Et_3PO can be attributed to an additive inductive contribution from the second C-bound *o*-carborane unit, which deepens the σ-hole and enhances the polar character of the Sb(1)–O(2) interaction. Notably, the $\Delta\delta$ value observed for **1b** exceeds that reported for closely related aryl-substituted stiboranes, consistent with the enhanced electron-withdrawing influence of a C-bound *o*-carboranyl substituent in this system. In contrast, while **2b** exhibits a similarly large $\Delta\delta$ value, the absence of a directly comparable perfluoroaryl analogue precludes a one-to-one comparison; nevertheless, the magnitude of the response supports a general trend of increased pnictogen acidity upon carborane substitution.[46] To probe whether the Lewis acidity trends inferred from the Gutmann–Beckett measurements translate into catalytic reactivity, we evaluated **1b** and **2b** as catalysts for the transfer hydrogenation of quinoline using a Hantzsch ester as the hydride source.[69,70] This reaction was selected as a well-established benchmark for assessing pnictogen-mediated Lewis acid catalysis under mild conditions using *in situ* ^{1}H NMR monitoring over 12 hours. Under these conditions, both **1b** and **2b** exhibited catalytic reactivity consistent with previously reported Sb(v) systems (see SI, S32 and S33).

Fluoride ion binding measurements

To further corroborate the Gutmann–Beckett measurement results, complementary fluoride-binding and computational acidity analyses were conducted. While the Guttman–Beckett method probes neutral donor interactions, Lewis acidity in pnictogen systems is often examined using anionic fluoride capture. Upon addition of fluoride, the antimony center can engage in a strong, quantifiable Sb(v)–F interaction that can be monitored and quantified by ^{19}F NMR spectroscopy. The magnitude of the ^{19}F NMR resonance shift corresponds to the magnitude of the Lewis acidity at the Sb(v) center.[47] Upon addition of 1 equiv. of $[^nBu_4N][Ph_3SiF_2]$ (TBAT) to **2b** in dichloromethane, the ^{19}F NMR resonance shifts downfield to −77.1 ppm (reference ^{19}F NMR resonance for TBAT = −98.5 ppm) which is consistent with previous studies on electrophilic Sb(v) compounds, overall implying the formation of a Sb(v)–F adduct.[48,49]

In comparison, **1b** exhibits a more downfield ^{19}F NMR signal near −58.6 ppm, indicating a stronger fluoride binding affinity. Slow vapor diffusion of TBAT-treated **1b** afforded diffraction-quality crystals of the corresponding fluoride adduct **1d**. X-ray crystallographic analysis of the μ^2-fluoride species reveals

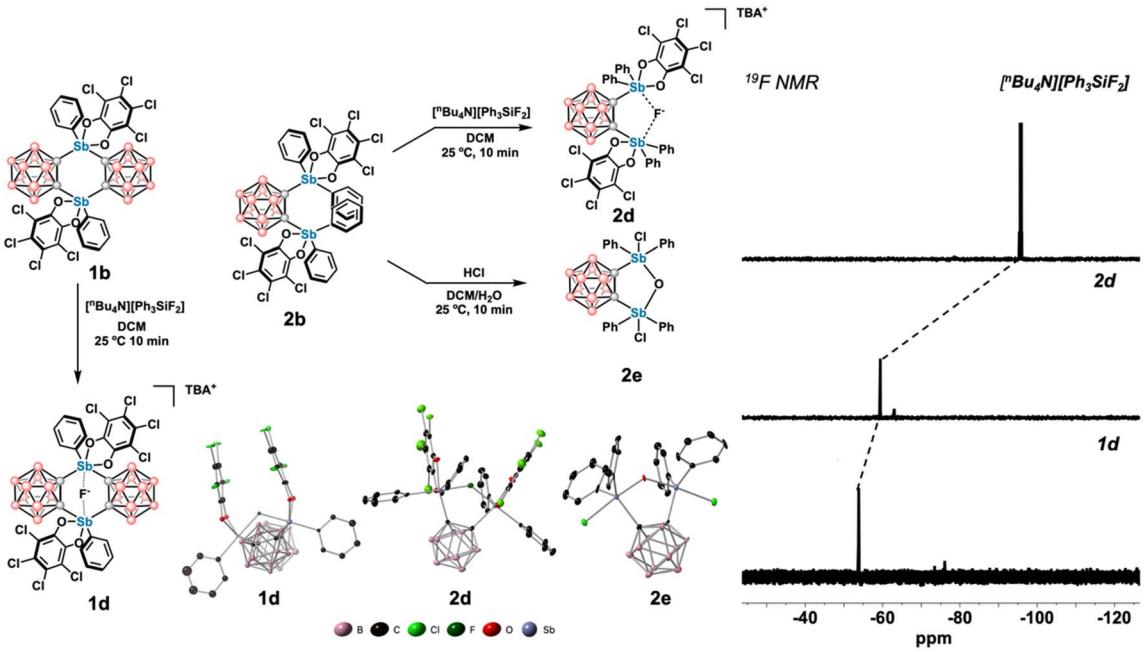

Fig. 4 Left: Fluoride-binding reactivity of Sb(v) complexes **1b** and **2b** with $[nBu_4N][Ph_3SiF_2]$, generating fluoride adducts **1d** and **2d**; hydrolysis of **2b** to organoantimony hydroxy species **2e**. Center: solid-state structures of **1d**, **2d**, and **2e**. Right: ^{19}F NMR spectra illustrating the distinct fluoride resonances observed for **1d** and **2d** upon reaction with 1 equiv. of $[nBu_4N][Ph_3SiF_2]$.

bridging Sb–F interactions with an average bond length of 2.159(6) Å and a highly bent Sb–F–Sb geometry (117.6(3)°), together with an elongated Sb–Sb distance of 3.691(1) Å. In contrast, the stibonium fluoride adduct reported by Gabbaï and co-workers displays a terminal Sb–F bond of 2.028 Å. The increased Sb–F distance and substantial angular compression observed in **1d** therefore highlight the unique ability of C-bound *o*-carboranyl substituents to support a μ^2-F bridging mode that is inaccessible to conventional tetraaryl stibonium systems, reinforcing the enhanced Lewis acidity and σ-hole delocalization imparted by the *bis*(carboranyl) scaffold. Consistent with the GB method, fluoride binding titrations reveal the same Lewis acidity order (**1b** > **2b**), emphasizing the enhanced Lewis acidity imparted by the attachment of two *o*-carboranyl scaffolds to Sb(v) centers. This convergence across orthogonal probes strengthens the interpretation that C-bound *o*-carborane substitution systematically enhances the accessible *σ*-hole depth and stabilizes Sb(v)–F interactions. Interestingly, during the course of our studies we have also observed that despite **1b** being more Lewis acidic than **2b**, it is not moisture sensitive. On the other hand, when **2b** is exposed to a mixture of acidified water in dichloromethane, a rapid reaction occurs, leading to the quantitative formation of the corresponding organoantimony hydroxy species in which an oxygen atom inserts between two antimony centers in a μ^2-oxo fashion (Fig. 4). The single crystal X-ray structure of **2e** shows a μ^2-oxo motif featuring Sb–O average distances of 1.976(6) Å and a bent Sb–O–Sb angle of 132.9(3)°, together with an elongated Sb–Sb separation of 3.610(1) Å, reflecting significant geometric distortion around the bridging oxygen. This bending places **2e** between the extremes observed in Sowerby's systems, which range from linear geometries (180°) in the *p*-tolyl derivative to a more acute 171.5° bridge in the *o*-tolyl analogue. The more compressed 132° angle in **2e** therefore indicates a stronger deviation from linearity than either aryl-substituted example, consistent with the greater steric and electronic demand imposed by the C-bound *o*-carborane substituent, which enforces a tighter Sb–O–Sb hinge and stabilizes the μ^2-oxo unit against hydrolytic degradation. Similar structures have been shown by Sowerby *et al.*, in which they prepared $(SbR_3Br)_2O$ where R is required to be a bulky *o*/*p*-tolyl group. Without bulky ligands to stabilize the Sb–O–Sb bridge, the degradation product results in an unhydrolyzed compound.[50] In this case, the bulky *o*-carborane clusters provide stability to the Sb–O–Sb to avoid this degradation. Importantly, these studies show that Sb(v)–C bonds with *o*-carborane substituents are hydrolytically stable under relatively forcing conditions.

To rationalize our experimental trend further, we conducted computational studies using dispersion-corrected density functional theory calculations (B3LYP-D3/LANL2Dz-def2-SVP in the gas phase; see SI, Table S3) and compared these results to a representative series of benchmark compounds recently introduced by Gabbaï and co-workers.[21] As shown in Fig. 5, replacing perfluorinated aryl groups with one (**2b**) or two (**1b**) C-bound *o*-carboranyl substituents produces a systematic increase in electron affinity, reflecting increasingly electron-deficient antimony centers.

From the computational findings, the addition of a second *o*-carboranyl unit further stabilizes the LUMO, which increases the *σ*-hole depth leading to stronger Lewis acidity (see SI, Table S1). The electrostatic potential surface of **2b** (Fig. 5B) further illustrates the emergence of a highly localized region of positive

B

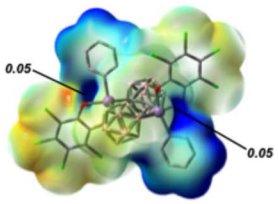

C

Compound	FIA [kJ mol^{-1}]	EA [eV]	LUMO [eV]
$C_6F_4[SbPh_2(o\text{-}C_6Cl_4O_2)]_2$	387.3	1.69	-2.12
2a	122.4	0.57	-1.788
1a	159.4	1.25	-1.880
2b	449.7	2.31	-2.53
1b	450.9	2.78	-3.13

D

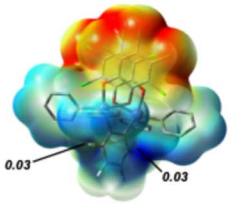

Fig. 5 (A) Comparison of benchmark perfluoroaryl-stabilized Sb(v) species (Gabbaï *et al.*, 2021) with C-bound mono- (**2b**) and *bis*(carboranyl) (**1b**) stiboranes, illustrating the trend of decreasing LUMO energies and increasing Lewis acidity across the series. (B) Electrostatic potential map of **1b** highlighting the surface potential of the deepened σ-hole at antimony. (C) Computed fluoride ion affinities (FIA), electron affinity (EA), and LUMO energies for reference and carborane-functionalized systems. (D) Electrostatic potential map of $Sb_2C_6F_4Ph_4oCl_2$ with surface potential values at each σ-hole.

potential, *i.e.* a deepened *σ*-hole, directed along the Sb–O bond, providing a visual representation of the inductive effect applied by the *o*-carboranyl framework. When compared with the perfluoroaryl analogue, $Sb_2C_6F_4Ph_4OCl_2$, the surface potential values are larger, indicative of a more electron deficient *σ*-hole (Fig. 5D). In addition, relative to the perfluoroaryl analogue, $Sb_2C_6F_4Ph_4OCl_2$ (FIA = 387 kJ mol^{-1}; EA = 1.69 eV), both carborane-functionalized systems display noticeably greater fluoride affinities, **1b** (448.2 kJ mol^{-1}, 2.78 eV) and **2b** (449.7 kJ mol^{-1}, 2.31 eV) indicating an enhanced capacity to engage hard Lewis bases. This trend is also mirrored in the computed hydrogen ion affinities (HIA), where both **1b** and **2b** exhibit substantially higher affinities than the perfluoroaryl analogue. However, the HIA values are not as pronounced as the FIA values demonstrating the hard nature of the antimony centers.[51] Both FIA and HIA calculations were done in the gas phase for better comparison with reported literature values as well as to reduce computational cost.[22] Notably, prior literature reports[51,52] suggest that if a solvation model was implemented, all FIA and HIA values generally see a decrease by roughly 100–200 kJ mol^{-1} due to solvent dampening of charge density. Although structure **1b** exhibits amplified Lewis acidity, a result of the highly stabilized LUMO orbitals, it should be noted that **1b** displays a slightly lower FIA value due to the secondary steric effects as a result of the icosahedral boron clusters. This is demonstrated by the fact that the bond lengths and bond angles between the antimony centers and the fluoride anion are all slightly larger than its counterpart, structure **2b** (see SI, S61–S70).[53] Together, these data are consistent with a strongly electron-withdrawing icosahedral boron cluster leading to an increase in the polar character of the antimony(v) acceptor sigma-hole site, culminating in a marked enhancement in computed Lewis acidity across the series. Taken together, these results demonstrate that *o*-carborane substitution of the classical perfluoroaryl groups, particularly in the C-bound carboranyl motif, amplifies Lewis acidity at the Sb(v) centers by simultaneously lowering frontier orbital energies and enforcing a rigid geometry. Examining the ^{19}F NMR titrations, rationalized by computational methods, together with ^{31}P NMR shifts from the GB method, provides a consistent ranking that validates the Lewis acidity strength order of **1b** and **2b**.

Conclusions

In this work, we introduced C-bound *o*-carborane as a powerful electron-withdrawing substituent for tuning the *σ*-hole depth at two antimony sites in a bridging moiety. Two *o*-carborane bridged stibanes were prepared (**1a** and **2a**) and cleanly oxidized to the corresponding Sb(v) stiboranes (**1b** and **2b**). Structural analysis confirmed conversion from trigonal pyramidal Sb(III) to distorted trigonal-bipyramidal Sb(v) in both systems while preserving the rigid carborane bridge that enforces large metalloid separations between antimony centers. Across independent acidity probes, including Gutmann–Beckett ($\Delta\delta^{31}$P), ^{19}F NMR spectroscopic fluoride binding measurements, and DFT-calculated FIA, *o*-carborane substitution increased Lewis

acidity relative to aryl benchmarks, with the *bis*(carboranyl) framework **1b** consistently exhibiting the strongest acidity in the series. Computed LUMO energies and FIA values correlate with the experimental trends, supporting a primarily σ-inductive origin for the effect. While C-based carborane substitution significantly enhances Sb(v) acidity, the present scaffolds do not reach the "superacid" regime by common FIA benchmarks, and replacement of all aryl substituents with C-bound carboranes is likely needed to achieve this goal (*e.g.*, *tris*(carboranyl)Sb system).

Overall, we show how *o*-carborane provides a lever for designing heavy-pnictogen Lewis acids whose strength and geometry can be tuned without sacrificing stability. Given their robust binding to oxo and fluoride donors, the platforms reported here are promising starting points for anion capture, halide- or oxide-abstraction, and σ-hole-assisted catalysis. More broadly, this work provides additional evidence that carboranes and, more generally, boron clusters can function as tunable substituents across a wide range of heteroatoms,[53–71] enabling precise modulation of their electronic properties. In this capacity, these clusters serve as compelling alternatives to traditional aryl- and alkyl-based substituents, offering access to electronic and structural features that are difficult to achieve using conventional organic frameworks.[71]

Author contributions

All authors have given approval to the final version of the manuscript.

Conflicts of interest

There are no conflicts to declare.

Data availability

Supplementary information (SI): methods description, characterization data for all new compounds, spectroscopic and computational data. See DOI: https://doi.org/10.1039/d6sc00316h.

CCDC 2514933–2514942 contain the supplementary crystallographic data for this paper.[72a–g]

Acknowledgements

A. M. S. thanks NIGMS MIRA 5R35GM124746 for supporting this work. O. G. thanks UCLA for start-up funds and NIGMS MIRA R35GM137797. The S10 program of the NIH Office of Research Infrastructure Programs, under grant S10OD028644, is acknowledged for the NEO600 in the NMR Facility at UCLA.

References

1 F. E. Paulik, S. I. E Green and R. E. Dessy, The preparation and study of some pentafluorophenylmercury compounds, *J. Organomet. Chem.*, 1965, **3**, 229, DOI: 10.1016/S0022-328X(00)87504-X.

2 (*a*) A. C. Massey, J. Park and F. G. A. Stone, Tris(pentafluorophenyl)boron, *Proc. Chem. Soc.*, 1963, 212, DOI: 10.1039/PS9630000189; (*b*) A. G. Massey and A. J. Park, Perfluorophenyl Derivatives of the Elements: I. Tris(Pentafluorophenyl)Boron, *J. Organomet. Chem.*, 1964, **2**(3), 245–250, DOI: 10.1016/S0022-328X(00)80518-5.

3 J. Lynch and M. F. Lappert, Perfluorophenyl-silicon compounds, *Chem. Commun.*, 1968, 750–751, DOI: 10.1039/C19680000750.

4 R. Grimes *Carboranes*, 3rd edn, Elsevier Inc., 2016.

5 T. Belgardt, J. Storre, H. W. Roesky, M. Noltemeyer and H.-G. Schmidt, Tris(Pentafluorophenyl)Alane: A Novel Aluminum Organyl, *Inorg. Chem.*, 1995, **34**(14), 3821–3822, DOI: 10.1021/ic00118a033.

6 X. Yang, C. B. Knobler and M. F. Hawthorne, "[12] Mercuracarborand-4", the First Representative of a New Class of Rigid Macrocyclic Electrophiles: The Chloride Ion Complex of a Charge-Reversed Analogue of [12]Crown-4, *Angew. Chem., Int. Ed.*, 1991, **30**, 1507–1508, DOI: 10.1002/anie.199115071.

7 X. Yang, C. B. Knobler, Z. Zheng and M. F. Hawthorne, Host-Guest Chemistry of a New Class of Macrocyclic Multidentate Lewis Acids Comprised of Carborane-Supported Electrophilic Mercury Centers, *J. Am. Chem. Soc.*, 1994, **116**(16), 7142–7159, DOI: 10.1021/ja00095a018.

8 (*a*) F. Teixidor, R. Núñez, C. Viñas, R. Sillanpää and R. Kivekäs, The Distinct Effect of the o-Carboranyl Fragment: Its Influence on the I–I Distance in R_3PI_2 Complexes, *Angew. Chem., Int. Ed.*, 2000, **39**, 4290–4292, DOI: 10.1002/1521-3773(20001201)39:23<4290::AID-ANIE4290>3.0.CO;2-3; (*b*) A. M. Spokoyny, C. D. Lewis, G. Teverovskiy and S. L. Buchwald, Extremely Electron-Rich, Boron-Functionalized, Icosahedral Carborane-Based Phosphinoboranes, *Organometallics*, 2012, **31**, 8478–8481, DOI: 10.1021/om301116x; (*c*) A. M. Spokoyny, C. W. Machan, D. J. Clingerman, M. S. Rosen, M. J. Wiester, R. D. Kennedy, C. L. Stern, A. A. Sarjeant and C. A. Mirkin, A Coordination Chemistry Dichotomy for Icosahedral Carborane-Based Ligands, *Nat. Chem.*, 2011, **3**(8), 590–596, DOI: 10.1038/nchem.1088; (*d*) H. A. Mills, C. G. Jones, K. P. Anderson, A. D. Ready, P. I. Djurovich, S. I. Khan, J. N. Hohman, H. M. Nelson and A. M. Spokoyny, Sterically Invariant Carborane-Based Ligands for the Morphological and Electronic Control of Metal–Organic Chalcogenolate Assemblies, *Chem. Mater.*, 2022, **34**, 6933–6943, DOI: 10.1021/acs.chemmater.2c01319; (*e*) K. Jaiswal, K. Chulsky, M. Gandelman and R. Dobrovetsky, o-Carboranylene *versus* Phenylene Backbones in Cyclization Reactions of 1,2 Diketones with Hydrosilanes, *Organometallics*, 2020, **39**(23), 4232–4237.

9 L. Jain, V. K. Jain, N. Kushwah, M. K. Pal, A. P. Wadawale, V. I. Bregadze and S. A. Glazun, Chalcogenocarboranes: A Family of Multifaceted Sterically Demanding Ligands, *Coord. Chem. Rev.*, 2014, **258–259**, 72–118, DOI: 10.1016/j.ccr.2013.09.003.

10 (*a*) M. Beau, S. Lee, S. Kim, W.-S. Han, O. Jeannin, M. Fourmigué, E. Aubert, E. Espinosa and I.-R. Jeon,

Strong σ-Hole Activation on Icosahedral Carborane Derivatives for a Directional Halide Recognition, *Angew. Chem., Int. Ed.*, 2021, **133**(1), 370–374, DOI: 10.1002/ange.202010462; (*b*) M. Sceney, K. F. White and J. L. Dutton, *Ortho*-Carborane-Supported Hypervalent Iodine(III) Reagents: A Scaffold for Enhanced Oxidative Capability, *J. Am. Chem. Soc.*, 2025, **147**, 32347–32351, DOI: 10.1021/jacs.5c10358.

11 (*a*) M. O. Akram, J. R. Tidwell, J. L. Dutton and C. D. Martin, Tris(ortho-carboranyl)borane: An Isolable, Halogen-Free, Lewis Superacid, *Angew. Chem., Int. Ed.*, 2022, **61**, e202212073, DOI: 10.1002/anie.202212073; (*b*) M. O. Akram, C. D. Martin and J. L. Dutton, The Effect of Carborane Substituents on the Lewis Acidity of Boranes, *Inorg. Chem.*, 2023, **62**, 13495–13504, DOI: 10.1021/acs.inorgchem.3c01872.

12 A. J. Baublis, T. A. Kerr, M. Gembicky and A. M. Spokoyny, Carboranes with Exopolyhedral Boron–Tetrel Bonds, *Organometallics*, 2025, **44**(20), 2394–2401, DOI: 10.1021/acs.organomet.5c00258.

13 (*a*) B. L. Murphy and F. P. Gabbaï, Binding, Sensing, And Transporting Anions with Pnictogen Bonds: The Case of Organoantimony Lewis Acids, *J. Am. Chem. Soc.*, 2023, **145**(36), 19458–19477, DOI: 10.1021/jacs.3c06991; (*b*) L. M. Lee, M. Tsemperouli, A. I. Poblador-Bahamonde, S. Benz, N. Sakai, K. Sugihara and S. Matile, Anion Transport with Pnictogen Bonds in Direct Comparison with Chalcogen and Halogen Bonds, *J. Am. Chem. Soc.*, 2019, **141**, 810–814, DOI: 10.1021/jacs.8b12554.

14 V. Nori, F. Pesciaioli, A. Sinibaldi, G. Giorgianni and A. Carlone, Boron-Based Lewis Acid Catalysis: Challenges and Perspectives, *Catalysts*, 2022, **12**(1), 5, DOI: 10.3390/catal12010005.

15 W. E. Piers and T. Chivers, Pentafluorophenylboranes: From Obscurity to Applications, *Chem. Soc. Rev.*, 1997, **26**(5), 345–354, DOI: 10.1039/CS9972600345.

16 X. Zhou and P. Xing, Beyond Halogen Bonding: σ-Hole Interactions, *Trends Chem*, 2025, 7(8), 460–473, DOI: 10.1016/j.trechm.2025.06.001.

17 C. B. Aakeröy, M. Baldrighi, J. Desper, P. Metrangolo and G. Resnati, Supramolecular Hierarchy among Halogen-Bond Donors, *Chem.–Eur. J.*, 2013, **19**(48), 16240–16247, DOI: 10.1002/chem.201302162.

18 G. Cavallo, P. Metrangolo, R. Milani, T. Pilati, A. Priimagi, G. Resnati and G. Terraneo, The Halogen Bond, *Chem. Rev.*, 2016, **116**(4), 2478–2601, DOI: 10.1021/acs.chemrev.5b00484.

19 (*a*) D. Jovanovic, M. Poliyodath Mohanan and S. M. Huber, Halogen, Chalcogen, Pnictogen, and Tetrel Bonding in Non-Covalent Organocatalysis: An Update, *Angew. Chem., Int. Ed.*, 2024, **63**(31), e202404823, DOI: 10.1002/anie.202404823; (*b*) N. Li, R. Qiu, X. Zhang, Y. Chen, S.-F. Yin and X. Xu, Strong Lewis Acids of Air-Stable Binuclear Triphenylantimony(V) Complexes and Their Catalytic Application in C–C Bond-Forming Reactions, *Tetrahedron*, 2015, **71**(25), 4275–4281, DOI: 10.1016/j.tet.2015.05.013; (*c*) S. S. Chitnis, A. P. M. Robertson, N. Burford, B. O. Patrick, R. McDonald and M. J. Ferguson, Bipyridine Complexes of E3+ (E = P, As, Sb, Bi): Strong Lewis Acids, Sources of E(OTf)3 and Synthons for EI and EV Cations, *Chem. Sci.*, 2015, **6**(11), 6545–6555, DOI: 10.1039/C5SC02423D; (*d*) R. A. Ugarte, D. Devarajan, R. M. Mushinski and T. W. Hudnall, Antimony(V) Cations for the Selective Catalytic Transformation of Aldehydes into Symmetric Ethers, α,β-Unsaturated Aldehydes, and 1,3,5-Trioxanes, *Dalton Trans.*, 2016, **45**(27), 11150–11161, DOI: 10.1039/C6DT02121B; (*e*) A. P. M. Robertson, S. S. Chitnis, H. A. Jenkins, R. McDonald, M. J. Ferguson and N. Burford, Establishing the Coordination Chemistry of Antimony(V) Cations: Systematic Assessment of $Ph_4Sb(OTf)$ and Ph3Sb(OTf)2 as Lewis Acceptors, *Chem.–Eur. J.*, 2015, **21**(21), 7902–7913, DOI: 10.1002/chem.201406469; (*f*) A. Gini, M. Paraja, B. Galmés, C. Besnard, A. I. Poblador-Bahamonde, N. Sakai, A. Frontera and S. Matile, Pnictogen-bonding catalysis: brevetoxin-type polyether cyclizations, *Chem. Sci.*, 2020, **11**, 7086–7091, DOI: 10.1039/D0SC02551H; (*g*) G. Renno, D. Chen, Q.-X. Zhang, R. M. Gomila, A. Frontera, N. Sakai, T. R. Ward and S. Matile, Pnictogen-Bonding Enzymes, *Angew. Chem., Int. Ed.*, 2024, **63**, e202411347, DOI: 10.1002/anie.202411347; (*h*) E. Chakraborty and R. Weiss, Organoantimony: a versatile main-group platform for pnictogen-bonding and redox catalysis, *Chem. Soc. Rev.*, 2025, **54**, 11379–11397, DOI: 10.1039/D3CS00332A.

20 M. Hirai and F. P. Gabbaï, Squeezing Fluoride out of Water with a Neutral Bidentate Antimony(V) Lewis Acid, *Angew. Chem., Int. Ed.*, 2015, **54**(4), 1205–1209, DOI: 10.1002/anie.201410085.

21 M. Hirai and F. P. Gabbaï, Lewis Acidic Stiborafluorenes for the Fluorescence Turn-on Sensing of Fluoride in Drinking Water at ppm Concentrations, *Chem. Sci.*, 2014, **5**(5), 1886–1893, DOI: 10.1039/C4SC00343H.

22 D. You, B. Zhou, M. Hirai and F. P. Gabbaï, Distiboranes Based on Ortho-Phenylene Backbones as Bidentate Lewis Acids for Fluoride Anion Chelation, *Org. Biomol. Chem.*, 2021, **19**(22), 4949–4957, DOI: 10.1039/D1OB00536G.

23 P. Erdmann and L. Greb, What Distinguishes the Strength and the Effect of a Lewis Acid: Analysis of the Gutmann-Beckett Method, *Angew. Chem., Int. Ed.*, 2022, **61**(4), e202114550, DOI: 10.1002/anie.202114550.

24 M. A. Beckett, G. C. Strickland, J. R. Holland and K. A. Sukumar Varma, Convenient n.m.r. Method for the Measurement of Lewis Acidity at Boron Centres: Correlation of Reaction Rates of Lewis Acid Initiated Epoxide Polymerizations with Lewis Acidity, *Polymer*, 1996, **37**(20), 4629–4631, DOI: 10.1016/0032-3861(96)00323-0.

25 V. I. Bregadze, N. N. Godovikov, A. N. Degtyarev and M. I. Kabachnik, The Synthesis of Tris(Methyl-*o*-Carboranyl)Phosphine, *J. Organomet. Chem.*, 1976, **112**(2), C25–C26, DOI: 10.1016/S0022-328X(00)80745-7.

26 W. V. Taylor, C. X. Cammack, S. A. Shubert and M. J. Rose, Thermoluminescent Antimony-Supported Copper-Iodo Cuboids: Approaching NIR Emission *via* High

Crystallographic Symmetry, *Inorg. Chem.*, 2019, **58**(24), 16330–16345, DOI: 10.1021/acs.inorgchem.9b00229.

27 S. S. Eaton and G. R. Eaton, Rotation of Phenyl Rings in Metal Complexes of Substituted Tetraphenylporphyrins, *J. Am. Chem. Soc.*, 1975, **97**(13), 3660–3666, DOI: 10.1021/ja00846a016.

28 K. Yang, F. Gallazzi, C. Arens and R. Glaser, Importance of Solvent-Bridged Structures of Fluorinated Diphenylalanines: Synthesis, Detailed NMR Analysis, and Rotational Profiles of Phe(2-F)-Phe(2-F), Phe(2-F)-Phe, and Phe-Phe(2-F), *ACS Omega*, 2022, **7**(46), 42629–42643, DOI: 10.1021/acsomega.2c06351.

29 H. Komber, K. Stumpe and B. Voit, The Rotation of Pentaphenylphenyl Groups and Their Terminal Phenyl Groups: A Variable-Temperature 1H NMR Study on an Albatrossene and a Three-Bladed Molecular Propeller, *Tetrahedron*, 2007, **48**(15), 2655–2659, DOI: 10.1016/j.tetlet.2007.02.079.

30 C. Jiang, E. Lee, J. Schaefer, M. W. Holtcamp, T.-P. Lin and F. P. Gabbaï, Pnictogen-Bonding Catalysis: Copolymerization of CO2 and Epoxides on Antimony(V) Platforms, *ACS Catal.*, 2025, 17882–17892, DOI: 10.1021/acscatal.5c03781.

31 J. E. Smith and F. P. Gabbaï, Are Ar_3SbCl_2 Species Lewis Acidic? Exploration of the Concept and Pnictogen Bond Catalysis Using a Geometrically Constrained Example, *Organometallics*, 2023, **42**(3), 240–245, DOI: 10.1021/acs.organomet.2c00565.

32 R. Liu, Z. Han, Y. Lu, Z. Xu and W. Zhu, Pentavalent Pnictogen Bonds Involving Triarylpnictogen Catecholates as Strong Lewis Acids: Crystallographic Survey and Theoretical Analysis, *Comput. Theor. Chem.*, 2025, **1248**, 115171, DOI: 10.1016/j.comptc.2025.115171.

33 O. Coughlin, T. Krämer and S. L. Benjamin, Cationic Triarylchlorostibonium Lewis Acids, *Organometallics*, 2023, **42**(5), 339–346, DOI: 10.1021/acs.organomet.2c00426.

34 M. Yang, D. Tofan, C.-H. Chen, K. M. Jack and F. P. Gabbaï, Digging the Sigma-Hole of Organoantimony Lewis Acids by Oxidation, *Angew. Chem., Int. Ed.*, 2018, **57**(42), 13868–13872, DOI: 10.1002/anie.201808551.

35 A. M. Christianson, A. Kim, B. L. Murphy and F. P. Gabbaï, Fluoride Binding by a Neutral Organoantimony(V) Lewis Acid Embedded within a Dibenzodithiophene Chromophore, *Z. Anorg. Allg. Chem.*, 2025, **651**(2), e202400170, DOI: 10.1002/zaac.202400170.

36 R. R. Holmes, R. O. Day, V. Chandrasekhar and J. M. Holmes, Pentacoordinated Molecules. 67. Formation and Structure of Cyclic Five-Coordinated Antimony Derivatives. The First Square-Pyramidal Geometry for a Bicyclic Stiborane, *Inorg. Chem.*, 1987, **26**(1), 157–163, DOI: 10.1021/ic00248a031.

37 A. N. Efremov and V. V. Sharutin, Triphenylantimony and Pentaphenylantimony as the Starting Compounds for the Synthesis of Antimony(V) Phenyl Derivatives. Structure of Triphenylantimony, Bis(3,4-Difluorobenzoato) Triphenylantimony and Tetraphenylantimony Carbonate, *Russ. J. Coord. Chem.*, 2023, **49**(1), 56–62, DOI: 10.1134/S1070328422700324.

38 P. Pyykkö and M. Atsumi, Molecular Single-Bond Covalent Radii for Elements 1-118, *Chem.–Eur. J.*, 2009, **15**(1), 186–197, DOI: 10.1002/chem.200800987.

39 S. M. S. Chitnis, A. P. Robertson, N. Burford, B. O. Patrick, R. McDonald, J. Ferguson and M. Bipyridine, Complexes of E^{3+} (E = P, As, Sb, Bi): Strong Lewis Acids, Sources of $E(OTf)_3$ and Synthons for E^{I} and E^{V} Cations, *Chem. Sci.*, 2015, **6**(11), 6545–6555, DOI: 10.1039/C5SC02423D.

40 U. Mayer, V. Gutmann and W. Gerger, The Acceptor Number - A Quantitative Empirical Parameter for the Electrophilic Properties of Solvents, *Monatsh. fur Chem*, 1975, **106**(6), 1235–1257, DOI: 10.1007/BF00913599.

41 H. Hirao, K. Omoto and H. Fujimoto, Lewis Acidity of Boron Trihalides, *J. Phys. Chem.*, 1999, **103**(29), 5807–5811, DOI: 10.1021/jp9908303.

42 A. R. Jupp, T. C. Johnstone and D. W. Stephan, The Global Electrophilicity Index as a Metric for Lewis Acidity, *Dalton Trans.*, 2018, **47**(20), 7029–7035, DOI: 10.1039/C8DT01699B.

43 M. M. Shmakov, S. A. Prikhod'ko, V. N. Panchenko, M. N. Timofeeva, V. V. Bardin, V. N. Parmon and N. Yu. Adonin, The Organoboron Compounds: Their Lewis Acidity and Catalytic Activity, *Catal. Rev.*, 2025, **67**(3), 497–543, DOI: 10.1080/01614940.2024.2334462.

44 A. Y. Timoshkin, The Field of Main Group Lewis Acids and Lewis Superacids: Important Basics and Recent Developments, *Chem.–Eur. J.*, 2024, **30**(1), e202302457, DOI: 10.1002/chem.202302457.

45 J. Schwarzmann, T. Eskelinen, S. Reith, J. Ramler, A. J. Karttunen, J. Poater and C. Lichtenberg, Bismuth as a Z-Type Ligand: An Unsupported Pt−Bi Donor-Acceptor Interaction and Its Umpolung by Reaction with H_2, *Angew. Chem., Int. Ed.*, 2024, **63**(41), e202410291, DOI: 10.1002/anie.202410291.

46 D. Tofan and F. P. Gabbaï, Fluorinated Antimony(V) Derivatives: Strong Lewis Acidic Properties and Application to the Complexation of Formaldehyde in Aqueous Solutions, *Chem. Sci.*, 2016, **7**(11), 6768–6778, DOI: 10.1039/C6SC02558G.

47 J. C. Haartz and D. H. McDaniel, Fluoride Ion Affinity of Some Lewis Acids, *J. Am. Chem. Soc.*, 1973, **95**(26), 8562–8565, DOI: 10.1021/ja00807a011.

48 L. T. Maltz and F. P. Gabbaï, Analyzing Fluoride Binding by Group 15 Lewis Acids: Pnictogen Bonding in the Pentavalent State, *Inorg. Chem.*, 2023, **62**(33), 13566–13572, DOI: 10.1021/acs.inorgchem.3c01987.

49 V. M. Gonzalez, G. Park, M. Yang and F. P. Gabbaï, Fluoride Anion Complexation and Transport Using a Stibonium Cation Stabilized by an Intramolecular PO → Sb Pnictogen Bond, *Dalton Trans.*, 2021, **50**(48), 17897–17900, DOI: 10.1039/D1DT03370K.

50 M. N. Gibbons and D. B. Sowerby, Multiply Bridged Organodiantimony(V) Compounds; Crystal structures of $[(SbR_2)_2(\mu\text{-}O)_2(\mu\text{-}O_2AsMe_2)_2]$ (R = Ph or p-Tolyl) and $[(SbR_3)_2(\mu\text{-}O)(\mu\text{-}O_2MR'_2)_2]$ (R = Ph,M = P, R′ = Me; R = Ph,M = As, R′ = Me or Ph;R = p-Tolyl, M = P,R′ = Me), *J. Chem. Soc., Dalton Trans.*, 1997, **16**, 2785–2792, DOI: 10.1039/A702244A.

51 M. Schorpp and I. Krossing, Soft Interactions with Hard Lewis Acids: Generation of Mono- and Dicationic Alkaline-Earth Metal Arene-Complexes by Direct Oxidation, *Chem. Sci.*, 2020, **11**(8), 2068–2076.

52 P. Erdmann, J. Leitner, J. Schwarz and L. Greb, An Extensive Set of Accurate Fluoride Ion Affinities for *P* -Block Element Lewis Acids and Basic Design Principles for Strong Fluoride Ion Acceptors, *ChemPhysChem*, 2020, **21**(10), 987–994.

53 H. Böhrer, N. Trapp, D. Himmel, M. Schleep and I. Krossing, From Unsuccessful H_2 -Activation with FLPs Containing $B(Ohfip)_3$ to a Systematic Evaluation of the Lewis Acidity of 33 Lewis Acids Based on Fluoride, Chloride, Hydride and Methyl Ion Affinities, *Dalton Trans.*, 2015, **44**(16), 7489–7499, DOI: 10.1039/C4DT02822H.

54 P.-F. Cui, Y. Gao, S.-T. Guo, Y.-J. Lin, Z.-H. Li and G.-X. Jin, Metalloradicals Supported by a meta-Carborane Ligand, *Angew. Chem., Int. Ed.*, 2019, **58**, 8129–8133, DOI: 10.1002/anie.201903467.

55 S. P. Fisher, S. G. McArthur, V. Tej, S. E. Lee, A. L. Chan, I. Banda, A. Gregory, K. Berkley, C. Tsay, A. L. Rheingold, G. Guisado-Barrios and V. Lavallo, Strongly Coordinating Ligands To Form Weakly Coordinating Yet Functional Organometallic Anions, *J. Am. Chem. Soc.*, 2020, **142**, 251–256, DOI: 10.1021/jacs.9b10234.

56 C. Zhang, J. Wang, W. Su, Z. Lin and Q. Ye, Synthesis, Characterization, and Density Functional Theory Studies of Three-Dimensional Inorganic Analogues of 9,10-Diboraanthracene - A New Class of Lewis Superacids, *J. Am. Chem. Soc.*, 2021, **143**, 8552–8558, DOI: 10.1021/jacs.1c03057.

57 H. A. Mills, F. Alsarhan, T.-C. Ong, M. Gembicky, A. L. Rheingold and A. M. Spokoyny, Icosahedral m-Carboranes Containing Exopolyhedral B–Se and B–Te Bonds, *Inorg. Chem.*, 2021, **60**, 19165–19174, DOI: 10.1021/acs.inorgchem.1c02981.

58 S. Yao, A. Kostenko, Y. Xiong, C. Lorent, A. Růžička and M. Driess, Changing the Reactivity of Zero- and Mono-Valent Germanium with a Redox Non-Innocent Bis(silylenyl)carborane Ligand, *Angew. Chem., Int. Ed.*, 2021, **60**, 14864–14868, DOI: 10.1002/anie.202103769.

59 C. Zhang, X. Liu, J. Wang and Q. Ye, A Three-Dimensional Inorganic Analogue of 9,10-Diazido-9,10-Diboraanthracene: A Lewis Superacidic Azido Borane with Reactivity and Stability, *Angew. Chem., Int. Ed.*, 2022, DOI: 10.1002/anie.202205506.

60 J. Schulz, R. Clauss, A. Kazimir, S. Holzknecht and E. Hey-Hawkins, On the Edge of the Known: Extremely Electron-Rich (Di)Carboranyl Phosphines, *Angew. Chem., Int. Ed.*, 2023, **62**, e202218648, DOI: 10.1002/anie.202218648.

61 C. N. Kona, R. Oku, S. Nakamura, M. Miura, K. Hirano and Y. Nishii, Aromatic Halogenation Using a Carborane Catalyst, *Chem*, 2024, **10**, 402–413, DOI: 10.1016/j.chempr.2023.10.006.

62 D. Bawari, D. Toami, K. Jaiswal and R. Dobrovetsky, Hydrogen Splitting at a Single Phosphorus Centre and Its Use for Hydrogenation, *Nat. Chem.*, 2024, **16**, 1261–1266, DOI: 10.1038/s41557-024-01569-y.

63 T. A. Kerr, Y. A. Nelson, N. A. Bernier and A. M. Spokoyny, An Electrochemical Strategy for Chalcogenation of the closo-Dodecaborate $(B_{12}H_{12})^{2-}$ Anion, *Inorg. Chem.*, 2025, **64**, 8845–8850, DOI: 10.1021/acs.inorgchem.5c00469.

64 J. R. Riffle, C. L. Jowers, S. Luna, M. D. Smith and D. V. Peryshkov, Non-Spectator Behavior of a Neutral Phosphine Ligand Driven by a Redox-Active Boron Cluster, *Chem. Sci.*, 2025, **16**, 15997–16003, DOI: 10.1039/D5SC04058B.

65 A. D. Ready, V. T. Raviprolu, T. A. Kerr, J. W. Treacy, M. L. Matsumoto, P. E. Hammer, E. M. Sletten, K. N. Houk and A. M. Spokoyny, Carboranes without Cage Carbons: closo-Dodecaborate Mimics of Neutral closo-Carboranes, *J. Am. Chem. Soc.*, 2025, **147**, 25478–25488, DOI: 10.1021/jacs.5c05637.

66 Q.-Q. Ma, P. Zhou, Y. Liu and Z. Xie, Chelating 1,2-Bis(2′-picolyl)-o-carborane as a Supporting Ligand for Pd-Catalyzed Selective B(3,6)–H Difunctionalization of o-Carboranes, *Inorg. Chem.*, 2025, **64**, 5707–5715, DOI: 10.1021/acs.inorgchem.5c00383.

67 V. T. Raviprolu, P. Farias, V. Carta, H. Harman and V. Lavallo, When the Ferrocene Analogy Breaks Down: Metallocene Transmetallation Chemistry, *Angew. Chem., Int. Ed.*, 2023, **62**(39), e202308359, DOI: 10.1002/anie.202308359.

68 V. T. Raviprolu, A. Gregory, I. Banda, S. G. McArthur, S. E. McArthur, W. A. Goddard, C. B. Musgrave and V. Lavallo, Confirmation of Breslow's Hypothesis: A Carbene Stable in Liquid Water, *Sci. Adv.*, 2025, **11**(15), eadr9681, DOI: 10.1126/sciadv.adr9681.

69 T. Itoh, K. Nagata, M. Miyazaki, H. Ishikawa, A. Kurihara and A. Ohsawa, A Selective Reductive Amination of Aldehydes by the Use of Hantzsch Dihydropyridines as Reductant, *Tetrahedron*, 2004, **60**(31), 6649–6655, DOI: 10.1016/j.tet.2004.05.096.

70 S. Benz, J. López-Andarias, J. Mareda, N. Sakai and S. Matile, Catalysis with Chalcogen Bonds, *Angew. Chem.*, 2017, **129**(3), 830–833, DOI: 10.1002/ange.201611019.

71 A. M. Spokoyny, New ligand platforms featuring boron-rich clusters as organomimetic substituents, *Pure Appl. Chem.*, 2013, **85**, 903–919, DOI: 10.1351/PAC-CON-13-01-13.

72 (*a*) CCDC 2514933, Experimental Crystal Structure Determination, 2026, DOI: 10.5517/ccdc.csd.cc2qdzw0; (*b*) CCDC 2514934: Experimental Crystal Structure Determination, 2026, DOI: 10.5517/ccdc.csd.cc2qdzx1; (*c*) CCDC 2514935: Experimental Crystal Structure Determination, 2026, DOI: 10.5517/ccdc.csd.cc2qdzy2; (*d*) CCDC 2514936: Experimental Crystal Structure Determination, 2026, DOI: 10.5517/ccdc.csd.cc2qdzz3; (*e*) CCDC 2514937: Experimental Crystal Structure

Determination, 2026, DOI: 10.5517/ccdc.csd.cc2qf006; (*f*) CCDC 2514938: Experimental Crystal Structure Determination, 2026, DOI: 10.5517/ccdc.csd.cc2qf017; (*g*) CCDC 2514939: Experimental Crystal Structure Determination, 2026, DOI: 10.5517/ccdc.csd.cc2qf028; (*h*) CCDC 2514940: Experimental Crystal Structure Determination, 2026, DOI: 10.5517/ccdc.csd.cc2qf039; (*i*) CCDC 2514941, Experimental Crystal Structure Determination, 2026, DOI: 10.5517/ccdc.csd.cc2qf04b; (*j*) CCDC 2514942, Experimental Crystal Structure Determination, 2026, DOI: 10.5517/ccdc.csd.cc2qf05c.